

Global microscopic calculations of odd-odd nuclei

D. E. Ward,¹ B. G. Carlsson,¹ P. Möller,^{1,2,*} and S. Åberg¹

¹*Mathematical Physics, Lund University, S-22100 Lund, Sweden*

²*Theoretical Division, Los Alamos National Laboratory, Los Alamos, New Mexico 87545, USA*



(Received 23 April 2019; revised manuscript received 17 June 2019; published 3 September 2019)

The macroscopic-microscopic finite-range droplet model is combined with a particle-rotor coupling model in order to systematically describe low-energy spectra of odd-odd nuclei. The odd proton and neutron are allowed to interact through effective nuclear forces representing the residual neutron-proton interaction. In particular, ground-state spins and parities are calculated and compared to data, where all 268 axially symmetric nuclei which have reliable spin and parity assignments in the Nubase 2016 database are considered. Using a residual neutron-proton interaction composed of both central and tensor terms the agreement with experimental ground-state spins and parities reaches 41% for spherical nuclei and 31% for deformed nuclei. The model is applied to study possible α -decay chains in superdeformed odd-odd nuclei, and Q_α values are calculated considering favored decay-paths as compared to ground-state paths.

DOI: [10.1103/PhysRevC.100.034301](https://doi.org/10.1103/PhysRevC.100.034301)

I. INTRODUCTION

It is a challenge to find models for nuclear structure properties all over the periodic system of even-even, odd-even, and odd-odd nuclei. Such models are reasonably based on a mean-field description with effective forces and parameters adjusted to experimental data. Existing efforts in terms of phenomenological macroscopic-microscopic models are indeed rather successful in the description of several nuclear structure properties, such as nuclear masses, ground-state spins, fission barriers, and decay rates, see, e.g., Refs. [1–3]. However, these models mainly consider even-even and odd-even nuclei; odd-odd nuclei are usually schematically treated without special consideration of the proton-neutron coupling mechanism.

A systematic description of the structure of odd-odd nuclei is indeed challenging, since it involves a detailed description of the low-energy interaction and also the coupling of the odd particles to the other nucleons. A proper understanding of the residual interaction between the neutrons and protons is indeed of general interest. This interaction plays a most important role in several theoretical models, e.g., for nuclear density functional theory based studies of weak processes such as β decay [4] and neutrino capture [5].

By combining the macroscopic-microscopic finite-range droplet model (FRDM) [1] with a particle-rotor model and a proper neutron-proton interaction we here calculate low-energy properties of odd-odd nuclei. The FRDM gives the most accurate results for ground-state spins of odd nuclei [2,6] which is a prerequisite for the extension to the odd-odd cases. Indeed, in recent calculations of ground-state spin/parity for odd nuclei the agreement with data is about 90% for spherical and 40% for deformed nuclei [2].

In deformed nuclei the coupling between the two odd particles and the core may be treated in the particle-rotor model [7–9]. The neutron-proton interaction plays an important role in the description of the low-energy structure, and we consider the δ interaction as well as finite-range Gaussian interactions with both central and tensor terms. Calculations with the different interactions are compared to data for the description of odd-odd spectra in spherical and deformed nuclei. In particular, we systematically calculate ground-state spin and parity and compare to available data.

We also discuss the spectrum of low-lying states in spherical and in axially deformed odd-odd nuclei. A particular challenge of today is the understanding and interpretation of α and γ decay of superheavy nuclei, in particular for odd-odd nuclei. When nuclear structure favors the α decay to excited states, γ decay to the ground state may reveal the detailed structure of the superheavy nuclei. We apply our model to the study of Q_α values for α -decay chains in odd-odd nuclei and note possible cases where decay to excited states may occur.

II. MODEL

The macroscopic-microscopic FRDM [1] gives a good global description of several ground-state properties. In particular, it gives a quite good reproduction of experimental spins and parities of the ground states of odd nuclei, as shown in Sec. II A. Therefore the FRDM is adopted as the starting point in this study of odd-odd nuclei. In this model the folded-Yukawa (FY) mean field is used for the microscopic calculation.

We determine the single-particle wave functions using the mean-field corresponding to the calculated ground-state shape in Ref. [1]. The pairing correlations are treated as in Ref. [1] through the Bardeen-Cooper-Schrieffer (BCS) method employing the approximate Lipkin-Nogami (LN) corrections. As

*Present address: Scientific Computing and Graphics Inc., Los Alamos, New Mexico 87544, USA.

a result we obtain an expansion of the single-particle wave functions in a cylindrical harmonic-oscillator basis, along with occupation numbers v_k^2 and quasiparticle energies E_k for each state k .

The simplest approach to determine spin and parity of the ground state of odd-odd nuclei is to couple the two spin vectors and let empirical rules determine the ground state, see Sec. IV A 1. below. However, we aim for a microscopic description of the coupling mechanism and the single-particle wave functions for protons and neutrons are therefore used in a two-quasiparticles-plus-rotor calculation where the residual interaction between the proton and neutron is taken into account. The two-quasiparticles-plus-rotor model is described in Sec. II B, and the residual neutron-proton interaction in Sec. II C. Some details of the calculations, for example, how spherical nuclei are treated, can be found in Sec. II D.

A. Ground states of odd- A nuclei

Before considering the odd-odd nuclei we revisit nuclei with odd particle numbers. As mentioned above, previous studies of ground-state spins I and parities π of odd- A nuclei lead to about 90% agreement for spherical and 40% agreement for deformed nuclei [2]. We repeat these calculations but with a slightly different recipe for determining the ground state I^π ; here the lowest-energy quasiparticle excitation of the odd-numbered species is used to determine the ground state. For the spherical case, the j -shell quantum number is used and for the deformed case the K^π quantum number of the quasiparticle.

Of the 681 odd- A , $Z \geq 8$, $N \geq 8$, nuclei with reliable I^π assignments in the Nubase 2016 database [10], the 631 nuclei predicted not to have octupole-deformed ground-state shapes in Ref. [1] are considered. We ignore possible triaxiality of the ground-state shape [11] and treat the nuclei as axially deformed with shapes specified by the calculated [1] shape parameters ε_2 , ε_4 , and ε_6 . Classifying the nuclei with $|\varepsilon_2| \leq 0.05$ as spherical and nuclei with $|\varepsilon_2| > 0.05$ as deformed gives 158 spherical and 473 deformed nuclei. The agreement of the ground state I^π is 84% (132/158) for spherical and 42% (200/473) for deformed nuclei. The result is shown in Fig. 1.

Combining the agreement for spherical and deformed nuclei we obtain an agreement with experiment in a total of 53% of the cases. Assuming a 53% chance of finding the correct spin of each particle species one could expect to obtain an agreement of $(53\%)^2 = 28\%$ for the odd-odd cases. However, as seen in Fig. 1 the probabilities are not uncorrelated since we obtain continuous regions in the nuclear chart where most of the predicted odd-even ground-state spins tend to agree with experiment. The emergence of such regions will likely increase the agreement with the data. Thus from the consideration of the odd- A nuclei one would expect to have a somewhat larger than 28% agreement in the odd-odd cases.

B. Two quasiparticles plus rotor

We consider the case of axial symmetry and model a proton and a neutron quasiparticle coupled to a collective core using

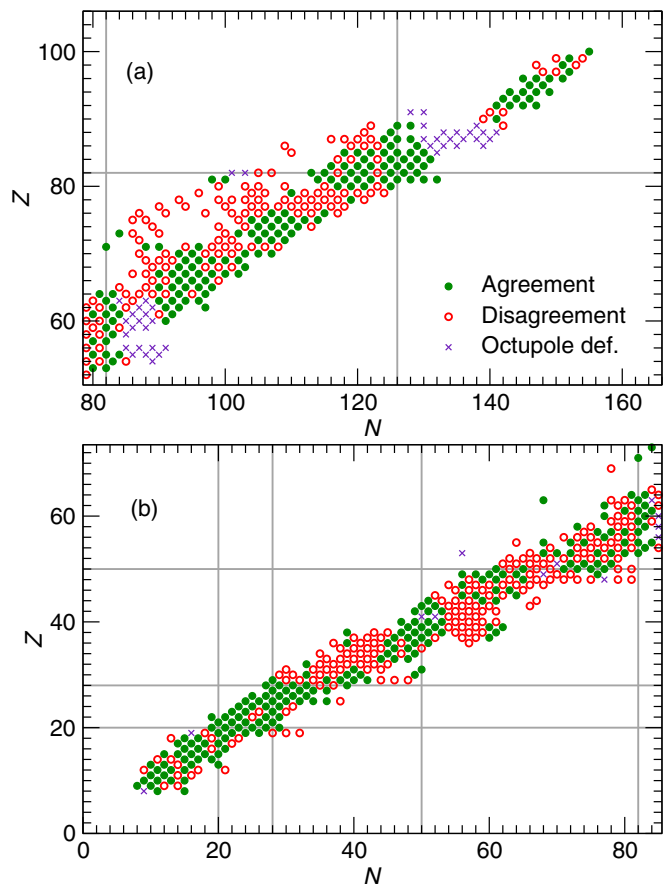


FIG. 1. Ground-state spin and parity for odd- A nuclei determined from the lowest-energy proton or neutron quasiparticle compared with data. Nuclei calculated to have an octupole deformed ground state are excluded from the comparison and marked with crosses.

the Hamiltonian operator [7–9]

$$H = H_{\text{col}} + H_{\text{qp}} + V_{pn}, \quad (1)$$

where H_{col} describes the collective rotation, H_{qp} the energies of the quasiparticles, and V_{pn} the residual proton-neutron interaction between the quasiparticles.

A Hamiltonian containing one- and two-body operators can be represented in terms of products of zero, two, and four quasiparticle operators [12]. For the collective rotation H_{col} , we include the two- and four-quasiparticle parts of the operator,

$$\mathcal{A}(R_1^2 + R_2^2) = \mathcal{A}[(I^2 - I_3^2) + (J^2 - J_3^2) - (I_+ J_- + I_- J_+)], \quad (2)$$

where $R_i = I_i - J_i$ is the angular momentum of the collective rotation, with $i = 1, 2$ denoting projection on one of the body-fixed axes perpendicular to the symmetry axis. $\vec{I} = (I_1, I_2, I_3)$ is the total angular momentum of the nucleus and $\vec{J} = (J_1, J_2, J_3)$ the total angular momentum in the intrinsic system.

The moment of inertia parameter

$$\mathcal{A} = \frac{1}{2\mathcal{J}_\perp}, \quad (3)$$

is expressed in terms of the moment of inertia perpendicular to the symmetry axis \mathcal{J}_\perp . The used model accounts for the decrease of the moment of inertia due to pairing and is chosen according to the prescription in Ref. [13].

The zero-quasi-particle part of Eq. (2) corresponds to the contribution from the vacuum $\mathcal{A}\langle 0|\mathcal{R}^2|0\rangle$, which would give a constant shift of all energies. This shift is neglected as it should already be accounted for in the ground-state binding energies in the FRDM.

H_{qp} is given by

$$H_{\text{qp}} = \sum_k E_k \beta_k^\dagger \beta_k, \quad (4)$$

where E_k are the LN-BCS quasiparticle energies in the FRDM.

The residual interaction between the proton and neutron quasiparticles V_{pn} is

$$V_{pn} = \frac{1}{4} \sum_{abcd} V_{abcd}^{22} \beta_a^\dagger \beta_b^\dagger \beta_d \beta_c, \quad (5)$$

where V_{abcd}^{22} contains antisymmetric matrix elements of the residual proton-neutron interaction \hat{V} (defined in the next subsection) and the BCS occupation numbers u, v for the quasiparticles a, b, c, d [12]. The zero- and two-quasiparticle terms originating from \hat{V} would affect the binding energies of even-even and odd- A nuclei and are not included since their contributions are assumed to be effectively incorporated in the mean field [9].

We employ the strong-coupling basis where the basis states consist of two-quasiparticle states in the intrinsic system coupled to the rotor. The states are symmetrized with respect to rotation around the one-axis. Taking into account the time-reversal symmetry gives two orthogonal groups of basis states,

$$|IMKn\rangle = \frac{1}{\sqrt{2}}(1 + e^{i\pi R_1})|IMK\rangle|np\rangle, \quad (6)$$

with $K = \Omega_n + \Omega_p \equiv K_>$, and

$$|IMKn\bar{p}\rangle = \frac{1}{\sqrt{2}}(1 + e^{i\pi R_1})|IMK\rangle|n\bar{p}\rangle, \quad (7)$$

with $K = |\Omega_n - \Omega_p| \equiv K_<$. Here $|np\rangle = \beta_n^\dagger \beta_p^\dagger |0\rangle$ is a two-quasiparticle state and

$$|IMK\rangle = \sqrt{\frac{2I+1}{8\pi^2}} \mathcal{D}_{MK}^{I*}(\omega) \quad (8)$$

is a normalized Wigner D function. $\Omega_{n(p)}$ is the total-angular momentum projection of the neutron (proton) quasiparticle $n(p)$ on the symmetry axis. $\bar{n}(\bar{p})$ indicates the time-reverse conjugate partner of the quasiparticle $n(p)$.

The intrinsic two-quasiparticle states that couple to the rotor

$$\beta_{k_n}^\dagger \beta_{k_p}^\dagger |0\rangle, \quad (9)$$

are formed by acting with Bogoliubov quasiparticle creation operators β_k^\dagger on the BCS vacuum $|0\rangle$, where β_k^\dagger creates a BCS quasiparticle in the FY single-particle orbital k . The vacuum $|0\rangle$ is constrained to have average particle numbers corresponding to the odd-odd nucleus.

C. Neutron-proton residual interaction

For the residual interaction between the neutron and proton we investigate three different forms: the δ interaction (Sec. II C 1) and two parametrizations of the Gaussian interaction (Sec. II C 2).

1. δ Interaction

The δ interaction has a simple form that allows fast numerical calculations. A central local interaction takes the form:

$$\hat{V} = (u_0 + u_1 \vec{\sigma}_p \cdot \vec{\sigma}_n) \delta(\vec{r}), \quad (10)$$

where $\vec{r} = \vec{r}_n - \vec{r}_p$. The interaction can be rewritten in terms of spin-isospin channels,

$$\hat{V} = \delta(\vec{r}) [G_{0t} \Pi_0^\tau \Pi_t^\sigma + G_{1s} \Pi_1^\tau \Pi_s^\sigma], \quad (11)$$

where $\Pi_{0(1)}^\tau$ projects on isospin-singlet (triplet) two-particle states, and $\Pi_{s(t)}^\sigma$ projects on spin-singlet (triplet) states. The transformation between the different notations can be written $G_{0t} = u_0 + u_1$ and $G_{1s} = u_0 - 3u_1$.

This leaves two free parameters in the interaction that we adjust to the $K_< \neq 0$ bandhead splittings in rare-earth nuclei given in Table I. These splittings are mainly sensitive to the difference $G_{0t} - G_{1s}$ and the choice $G_{0t} = -900$ and $G_{1s} = -300 \text{ MeV fm}^3$ lies in a region of values where the rms deviation from experiment is the smallest. In the following this interaction will be denoted “ δ .”

2. Gaussian interactions

A more realistic interaction is the Gaussian [14],

$$\hat{V} = V(r) \left[u_0 + u_1 \vec{\sigma}_p \cdot \vec{\sigma}_n + u_2 P_M + u_3 P_M \vec{\sigma}_p \cdot \vec{\sigma}_n + u_t \frac{S_{12}}{3} + u_{tm} P_M \frac{S_{12}}{3} + u_e^s \vec{l} \cdot \vec{s} + u_o^s P_M \vec{l} \cdot \vec{s} \right], \quad (12)$$

where $V(r)$ is a Gaussian,

$$V(r) = e^{-r^2/\mu^2}, \quad (13)$$

P_M is the space-exchange operator, and S_{12} is the tensor operator,

$$S_{12} = \frac{3}{r^2} (\vec{\sigma}_1 \cdot \vec{r})(\vec{\sigma}_2 \cdot \vec{r}) - \vec{\sigma}_1 \cdot \vec{\sigma}_2 = \sqrt{4\pi} \sqrt{6} [[\sigma^{(1)}, \sigma^{(2)}]_2, Y_2(\hat{r})]_0. \quad (14)$$

\vec{l} denotes the relative angular momentum,

$$\vec{l} = \vec{r} \times \vec{p} = (\vec{r}_n - \vec{r}_p) \times \frac{1}{2}(\vec{p}_n - \vec{p}_p), \quad (15)$$

and $\vec{s} = \vec{s}_p + \vec{s}_n$ is the total intrinsic spin of the two nucleons. Expressed in spin-isospin channels this interaction becomes

$$\hat{V} = V(r) [G_{1t} \Pi_1^\tau \Pi_t^\sigma + G_{0t} \Pi_0^\tau \Pi_t^\sigma + G_{1s} \Pi_1^\tau \Pi_s^\sigma + G_{0s} \Pi_0^\tau \Pi_s^\sigma + (G_{0t}^T \Pi_0^\tau \Pi_t^\sigma + G_{1t}^T \Pi_1^\tau \Pi_t^\sigma) S_{12} + (G_{0t}^{ls} \Pi_0^\tau \Pi_t^\sigma + G_{1t}^{ls} \Pi_1^\tau \Pi_t^\sigma) \vec{l} \cdot \vec{s}], \quad (16)$$

TABLE I. Bandhead splittings in rare-earth nuclei, $\Delta E = E_{K_>} - E_{K_<}$, where $E_{K_>}$ ($E_{K_<}$) is the excitation energy of the bandhead interpreted as the two quasiparticles coupled to projection $K_> = \Omega_n + \Omega_p$ ($K_< = |\Omega_n - \Omega_p|$). The category 1 (well-confirmed levels in low-energy spectra) data in Table 3 in Ref. [14] is used, denoted as expt. The results from Folded-Yukawa quasiparticles-plus-rotor calculations with different residual interactions are labeled: δ , contact interaction; 2, Covello Gaussian residual interaction; 3, Alexa Gaussian residual interaction. All energies in keV.

Z	N	A	p	n	$s_p s_n$	$K_>$	$K_<$	$E_{K_>}^{(\text{expt})}$	$E_{K_<}^{(\text{expt})}$	$\Delta E^{(\text{expt})}$	$\Delta E^{(\text{th},\delta)}$	$\Delta E^{(\text{th},2)}$	$\Delta E^{(\text{th},3)}$
65	93	158	[4 1 1]3/2+	[5 2 1]3/2-	$\uparrow\uparrow$	3	0	0	110	-110	72	-138	-149
65	95	160	[4 1 1]3/2+	[5 2 1]3/2-	$\uparrow\uparrow$	3	0	0	79	-79	85	-128	-137
65	95	160	[4 1 1]3/2+	[5 2 3]5/2-	$\uparrow\downarrow$	4	1	258	64	194	111	161	67
65	95	160	[4 1 1]3/2+	[6 4 2]5/2+	$\uparrow\uparrow$	4	1	64	139	-75	-67	-103	-62
67	97	164	[5 2 3]7/2-	[4 0 0]1/2+	$\uparrow\uparrow$	4	3	833	925	-92	-61	-95	-45
67	97	164	[5 2 3]7/2-	[4 0 2]3/2+	$\uparrow\downarrow$	5	2	733	620	113	84	148	35
67	97	164	[5 2 3]7/2-	[5 2 3]5/2-	$\uparrow\downarrow$	6	1	191	0	191	267	213	-84
67	99	166	[5 2 3]7/2-	[6 3 3]7/2+	$\uparrow\uparrow$	7	0	5	0	5	64	-237	-171
67	99	166	[5 2 3]7/2-	[5 2 1]1/2-	$\uparrow\downarrow$	4	3	372	191	181	124	128	-0
69	99	168	[4 1 1]1/2+	[6 3 3]7/2+	$\downarrow\uparrow$	4	3	148	0	148	74	114	33
69	99	168	[5 4 1]1/2-	[6 3 3]7/2+	$\downarrow\uparrow$	4	3	337	200	137	244	-38	-627
69	101	170	[4 1 1]1/2+	[5 1 2]5/2-	$\downarrow\uparrow$	3	2	447	204	243	242	214	118
71	103	174	[4 0 4]7/2+	[5 2 1]1/2-	$\downarrow\downarrow$	4	3	365	433	-68	-37	-81	-77
71	103	174	[4 0 4]7/2+	[5 2 1]3/2-	$\downarrow\uparrow$	5	2	1312	1185	127	106	77	100
71	103	174	[4 0 4]7/2+	[5 1 2]5/2-	$\downarrow\uparrow$	6	1	170	0	170	125	208	100
71	103	174	[5 4 1]1/2-	[5 1 2]5/2-	$\downarrow\uparrow$	3	2	414	278	136	-53	-78	-67
71	103	174	[5 3 0]1/2-	[5 1 2]5/2-	$\uparrow\uparrow$	3	2	1262	1293	-31	7	-55	-85
71	105	176	[4 0 4]7/2+	[5 1 0]1/2-	$\downarrow\uparrow$	4	3	791	662	129	64	163	83
71	105	176	[4 0 4]7/2+	[5 1 4]7/2-	$\downarrow\downarrow$	7	0	0	241	-241	113	-281	-305
71	105	176	[4 0 4]7/2+	[6 2 4]9/2+	$\downarrow\uparrow$	8	1	404	198	206	186	207	15
73	109	182	[4 0 4]7/2+	[5 1 0]1/2-	$\downarrow\uparrow$	4	3	114	0	114	73	137	89
73	109	182	[4 0 4]7/2+	[5 1 2]3/2-	$\downarrow\downarrow$	5	2	173	270	-97	-50	-123	-105
73	109	182	[4 0 4]7/2+	[5 0 3]7/2-	$\downarrow\uparrow$	7	0	777	584	193	241	292	21
73	109	182	[5 1 4]9/2-	[5 1 0]1/2-	$\uparrow\uparrow$	5	4	16	150	-134	-89	-144	-28
75	111	186	[4 0 2]5/2+	[5 1 0]1/2-	$\uparrow\uparrow$	3	2	99	211	-112	-64	-102	-5
75	111	186	[4 0 2]5/2+	[5 1 2]3/2-	$\uparrow\downarrow$	4	1	174	0	174	208	217	17
75	111	186	[4 0 2]5/2+	[5 0 3]7/2-	$\uparrow\uparrow$	6	1	186	316	-130	-209	-232	-344
75	113	188	[4 0 2]5/2+	[5 1 0]1/2-	$\uparrow\uparrow$	3	2	169	257	-88	-55	-92	-31
75	113	188	[4 0 2]5/2+	[5 1 2]3/2-	$\uparrow\downarrow$	4	1	183	0	183	157	169	19
75	113	188	[4 0 2]5/2+	[5 0 3]7/2-	$\uparrow\uparrow$	6	1	172	291	-119	-204	-218	-338

where the transformation between the different notations is shown in Table II. This interaction is thus a general nucleon-nucleon pn interaction consisting of a central part, noncentral tensor part, and a spin-orbit part.

For the Gaussian form of the interaction we consider two different parametrizations. In Ref. [15] a Gaussian np

interaction was fitted to spherical states in ^{210}Bi . In the following this parametrization will be denoted ‘‘Alexa.’’ As an alternative we also employ the effective interaction of Ref. [16] that was fitted to bandhead splittings in rare-earth nuclei [14]. In the following this parametrization will be denoted ‘‘Covello.’’ The parameters of the residual interactions are summarized in Table III.

D. Details of the calculations

Nuclei with ground-state quadrupole deformations larger than $|\varepsilon_2| > 0.05$ are treated as deformed. For well-deformed nuclei we expect that the residual interaction does not introduce significant mixing between rotational bands. We thus only include the diagonal matrix elements of V_{pn} in the strong-coupling basis. This leads to considerably fewer two-body matrix elements that need to be computed. The particles-plus-rotor calculations are performed in the basis obtained from all unique combinations of a neutron and a proton quasi particle,

TABLE II. Transformation expressing the interaction in spin-isospin channels.

$G_{0s}=u_0 - 3u_1 - u_2 + 3u_3$
$G_{0t}=u_0 + u_1 + u_2 + u_3$
$G_{1s}=u_0 - 3u_1 + u_2 - 3u_3$
$G_{1t}=u_0 + u_1 - u_2 - u_3$
$G_{0t}^T=(u_t + u_{tm})/3$
$G_{1t}^T=(u_t - u_{tm})/3$
$G_{0t}^s=u_e^s + u_o^s$
$G_{1t}^s=u_e^s - u_o^s$

TABLE III. Parameters of the effective interactions employed; μ is in fm, the strengths for the δ interaction in MeV fm³, and the rest in MeV.

	δ	Covello	Alexa
μ	—	1.4	1.4
G_{0s}	—	60.3	-1.80
G_{0r}	-900	-16.7	-75.6
G_{1s}	-300	9.7	-62.8
G_{1r}	—	-33.3	-10.6
G_{0r}^T	—	-41.0	-60.333
G_{1r}^T	—	4.33	11.667
G_{0r}^s	—	0	24
G_{1r}^s	—	0	-46

chosen from the 10 lowest energy neutron and proton qps, and their time-reversed states.

When the predicted ground-state quadrupole deformation is small, $|\varepsilon_2| \leq 0.05$, the nucleus is classified as spherical. For these cases the single-particle calculation is performed with a spherical mean field. To obtain the multiplets in the spherical system, the particles + rotor calculations are performed with a very small moment of inertia \mathcal{J}_\perp , giving a large moment of inertia parameter \mathcal{A}_{sph} . The term $\mathcal{A}_{\text{sph}}(R_1^2 + R_2^2)$ in Eq. (2) then acts as a quadratic constraint, pushing states with significant collective rotation $\langle \bar{R}^2 \rangle$ high up in energy. Due to the limited basis, the lowest eigenstates will have small nonzero expectation values of the collective-rotation angular momentum $\langle \bar{R}^2 \rangle$. States with $\langle H_{\text{col}} \rangle / \mathcal{A}_{\text{sph}} < 0.1$ are used as approximate eigenstates of the spherical system, with energies E' ,

$$E' = E - \langle H_{\text{col}} \rangle. \quad (17)$$

In the calculations $\mathcal{A}_{\text{sph}} = 500$ MeV is used. The sensitivity to the choice of \mathcal{A}_{sph} is tested for the case ²⁰⁸Bi with the δ interaction: Doubling \mathcal{A}_{sph} gives the same E' spectra to within 0.02 MeV. The spherical calculations are performed using the basis obtained by including the seven lowest-energy quasiparticle states for both protons and neutrons. All matrix elements of the residual interaction in this basis are taken into account.

For deformed as well as spherical nuclei, all matrix elements of the collective rotation H_{col} are taken into account. The two-body operator $\bar{R}^2 = (\vec{I} - \vec{J})^2$ is treated exact using analytic properties of the cylindrical oscillator basis [17].

III. ODD-ODD SPECTRA

In this section we test the model by investigating low-energy spectra of odd-odd nuclei. Not only the ground state but also the ordering and excitation energies of low-lying states depend on the residual proton-neutron interaction. Bandhead energy splitting in deformed nuclei, and the structure of multiplets in spherical nuclei, are two observables that are particularly sensitive to the residual interaction. These two properties are investigated in Sec. III A and in Sec. III B, respectively. The description of rotational bands

and low-energy spectra in deformed odd-odd nuclei is studied in more detail in Sec. III C.

A. Bandhead splittings

In deformed axially symmetric odd-odd nuclei two bandheads emerge with the angular momentum of the two coupled odd particles, namely $K_> = K_n + K_p$ and $K_< = |K_n - K_p|$, where $K_p(K_n)$ denotes the projection of the odd proton (neutron) angular momentum on the symmetry axis. The energy splitting $\Delta E = E_{K_>} - E_{K_<}$ between the two states is sensitive to the pn interaction, as well as to the rotational R^2 terms in Eq. (1). To test the different interactions we compare with experimental data for bandhead splittings in the rare-earth region [14] and actinide region [18]. Of the data set listed in Table 3 of Ref. [14] we select the well-confirmed levels in low-energy spectra. These are listed in Table I. For the actinides, we select the bandheads where both $K_>$ and $K_<$ configurations are identified with asymptotic Nilsson quantum numbers in Ref. [18], giving the data in Table IV.

The rotational contribution to ΔE is to first order $\mathcal{A}(K_> - K_<)$, with typical values for the moment of inertia parameter $\mathcal{A} \sim 10$ keV for the nuclei considered. In some earlier studies, e.g., Ref. [14], procedures to remove the rotational contribution from the experimental data and isolate the matrix elements of the residual interaction are employed. We choose not to adopt this approach, as it introduces some model dependence in the data, but rather compare calculated values directly with the experimental observable ΔE .

The bandhead splittings obtained using the three different residual interactions are shown in the rightmost columns of Tables I and IV. The root-mean-square (rms) deviations from experiment are summarized in Table V.

The δ interaction, which is adjusted to the $K_< \neq 0$ data for the rare-earth nuclei, gives the smallest rms for the $K_< \neq 0$ splittings for both rare-earth and actinide data. On the other hand, it gives a poor description of the $K_< = 0$ data.

The interaction between the odd proton and the odd neutron gives rise to an additional diagonal term in the strong-coupling basis for $K = 0$ states, called the Newby term [19]. Several studies [16] show that the δ interaction cannot reproduce the required Newby matrix elements, while simultaneously producing reasonable matrix elements for $K_< \neq 0$ splittings.

Of the two Gaussian interactions, we find that the Covello interaction gives the best description of the bandhead splittings. The description of the $K_< = 0$ bandhead splittings is significantly improved compared to the δ interaction, while the remaining data are described with a similar rms as with the δ , giving the overall best agreement. The Covello parametrization of the Gaussian interaction gives the correct bandhead lowest in energy for all cases except for three cases: the lowest lying bandhead in ¹⁶⁶Ho₉₉, the first excited in ¹⁶⁸Tm₉₉, and the first excited in ¹⁷⁴Lu₁₀₃. In these three cases data give $K_<$ as the lowest-lying bandhead, while the Covello interaction gives the $K_>$ bandhead as lowest. Excluding these three cases from all 45 cases considered in Tables I and IV decreases the rms for the Covello interaction from 66 to 44 keV.

TABLE IV. Similar to Table I but for bandheads in actinide nuclei. The experimental data are taken from Ref. [18].

Z	N	A	p	n	$s_p s_n$	$K_>$	$K_<$	$E_{K_>}^{(\text{exp})}$	$E_{K_<}^{(\text{exp})}$	$\Delta E^{(\text{exp})}$	$\Delta E^{(\text{th},\delta)}$	$\Delta E^{(\text{th},2)}$	$\Delta E^{(\text{th},3)}$
91	143	234	[5 3 0]1/2-	[7 4 3]7/2-	$\uparrow\uparrow$	4	3	0	74	-74	-54	-78	-25
91	143	234	[5 3 0]1/2-	[6 3 1]1/2+	$\uparrow\downarrow$	1	0	162	70	92	199	154	-12
91	145	236	[5 3 0]1/2-	[6 3 1]1/2+	$\uparrow\downarrow$	1	0	111	2	109	211	158	-11
93	143	236	[6 4 2]5/2+	[7 4 3]7/2-	$\uparrow\uparrow$	6	1	0	60	-60	-141	-93	-159
93	145	238	[6 4 2]5/2+	[6 3 1]1/2+	$\uparrow\downarrow$	3	2	87	0	87	49	85	26
93	145	238	[5 2 3]5/2-	[6 3 1]1/2+	$\downarrow\downarrow$	3	2	136	183	-47	-33	-80	-59
93	145	238	[5 3 0]1/2-	[6 3 1]1/2+	$\uparrow\downarrow$	1	0	374	218	156	216	162	-1
95	145	240	[5 2 3]5/2-	[6 3 1]1/2+	$\downarrow\downarrow$	3	2	0	53	-53	-35	-82	-59
95	145	240	[5 2 3]5/2-	[5 0 1]1/2-	$\downarrow\downarrow$	3	2	973	1016	-43	-25	-60	-40
95	147	242	[5 2 3]5/2-	[6 2 2]5/2+	$\downarrow\uparrow$	5	0	49	44	5	132	64	-92
95	147	242	[5 2 3]5/2-	[6 3 1]1/2+	$\downarrow\downarrow$	3	2	244	293	-48	-36	-84	-61
95	147	242	[5 2 3]5/2-	[6 2 0]1/2+	$\downarrow\uparrow$	3	2	902	874	28	122	121	-15
95	147	242	[5 2 3]5/2-	[5 0 1]1/2-	$\downarrow\downarrow$	3	2	975	1011	-36	-26	-60	-40
95	147	242	[6 4 2]5/2+	[6 3 1]1/2+	$\uparrow\downarrow$	3	2	388	356	32	51	83	27
95	149	244	[5 2 3]5/2-	[6 2 4]7/2+	$\downarrow\downarrow$	6	1	0	176	-176	-191	-128	-289
95	149	244	[5 2 3]5/2-	[6 2 2]5/2+	$\downarrow\uparrow$	5	0	365	336	29	136	71	-86
95	149	244	[5 2 3]5/2-	[6 3 1]1/2+	$\downarrow\downarrow$	3	2	421	485	-64	-36	-85	-61
95	149	244	[5 2 3]5/2-	[6 2 0]1/2+	$\downarrow\uparrow$	3	2	807	786	21	82	83	27
97	153	250	[6 3 3]7/2+	[6 1 3]7/2+	$\uparrow\uparrow$	7	0	86	216	-130	-71	-63	-42
97	153	250	[5 2 1]3/2-	[6 2 0]1/2+	$\uparrow\uparrow$	2	1	0	104	-104	-96	-130	-58
97	153	250	[6 3 3]7/2+	[6 2 0]1/2+	$\uparrow\uparrow$	4	3	36	115	-80	-37	-77	-41
97	153	250	[5 2 1]3/2-	[6 1 3]7/2+	$\uparrow\uparrow$	5	2	97	146	-49	-31	-92	-95
97	153	250	[6 3 3]7/2+	[6 2 2]3/2+	$\uparrow\downarrow$	5	2	316	212	105	60	100	31
97	153	250	[6 3 3]7/2+	[7 6 1]1/2-	$\uparrow\downarrow$	4	3	566	526	40	73	99	-19

In general, the Alexa interaction, which is fitted to spherical multiplet energies in ^{210}Bi [15], performs the worst of the three tested interactions.

B. Multiplets in spherical nuclei

The results for spherical multiplets in $^{210,208}\text{Bi}$, ^{90}Y , and ^{50}Sc using the three different residual interactions are com-

TABLE V. The rms deviation of theoretical bandhead splittings $\Delta E^{(\text{th})}$ and the corresponding experimental values $\Delta E^{(\text{exp})}$ in Tables I and IV. The first column describes the subset of data points considered, n is the number of data in the subset, and the remaining three columns contain the rms deviation in keV.

Set	n	rms (keV)		
		δ	Covello	Alexa
All	54	84	66	149
$K_< = 0$	11	150	90	117
$K_< \neq 0$	43	56	58	156
Rare earth	30	99	79	189
$K_< = 0$	5	196	121	118
$K_< \neq 0$	25	65	68	201
Actinide	24	60	43	72
$K_< = 0$	6	97	52	116
$K_< \neq 0$	18	40	40	50

pared with experimental data in Fig. 2. The δ interaction provides a good description of multiplet splittings, especially in the Bi isotopes, except for the $I^\pi = 0^-$ state in ^{210}Bi . For the two lighter nuclei ^{90}Y and ^{50}Sc the δ interaction gives good results. The correct ground-state spin is predicted correctly in all cases except for ^{210}Bi .

The Alexa Gaussian interaction gives a good description of $^{210,208}\text{Bi}$ and a fair description for the multiplets in lighter ^{90}Y and ^{50}Sc nuclei. This interaction was fitted to multiplets in ^{210}Bi , giving excellent agreement with data in Ref. [15]. In the present calculations with FY quasiparticles the energy of the $I^\pi = 0^-$ state in ^{210}Bi is overestimated. Performing the calculations with pure oscillator single-particle wave functions, as used in the original fit of the interaction, give energies more similar to the experimental data. In all cases the Alexa interaction predicts the correct ground-state spin.

The Covello Gaussian interaction captures the overall I dependence of the energies in the multiplets for all four nuclei but does not produce the correct I staggering. However, with the overall trends correct the ground state comes out right in all cases.

We also compare our result for ^{210}Bi and ^{50}Sc to a more sophisticated microscopic calculation where multiplets are calculated based on the pn-QRPA approach starting from a Skyrme force with addition of a separable Gaussian interaction (denoted Carlsson in Fig. 2) [20]. As seen for the $I = 0^-$ state in ^{210}Bi the finite-range Gaussian pushes the state up in energy compared to the δ interaction but not enough to obtain the correct ground state.

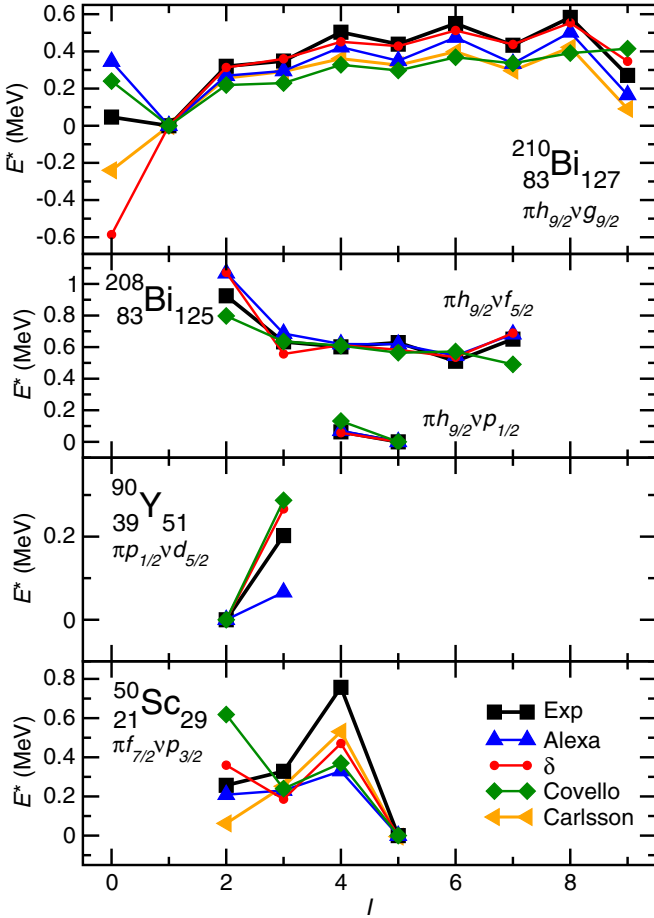


FIG. 2. Low-lying multiplets in the spherical nuclei $^{210,208}\text{Bi}$, ^{90}Y , and ^{50}Sc using different residual interactions V_{pn} . E^* denotes the excitation energy relative to the experimental ground-state configuration, and I is the spin.

The $I^\pi = 0^-$ state in ^{210}Bi is a spin triplet configuration, and the strong G_{0r} term of the δ interaction sets this state lowest in energy. The tensor terms included in the two Gaussian interactions are needed to push this state up in energy to obtain the correct $I^\pi = 1^-$ ground state. Of the four forces tested, it is only the forces with more complicated tensor components that are able to obtain the correct ordering between the $I^\pi = 1^-$ and $I^\pi = 0^-$ states.

The present many-body treatment takes into account the angular-momentum coupling and the interaction between the odd proton and the odd neutron. Taking the description a step further could include treating the coupling of the odd particles to vibrational modes of the remaining core in a particle-vibration coupling approach (PVC). As always, the effective interaction employed is intimately linked to the many-body treatment and a more refined PVC description could result in modifications of the effective interaction in particular concerning the tensor part [21,22].

C. Rotational bands in deformed nuclei

In Fig. 3 results from calculations with the Covello proton-neutron interaction are compared to 11 different

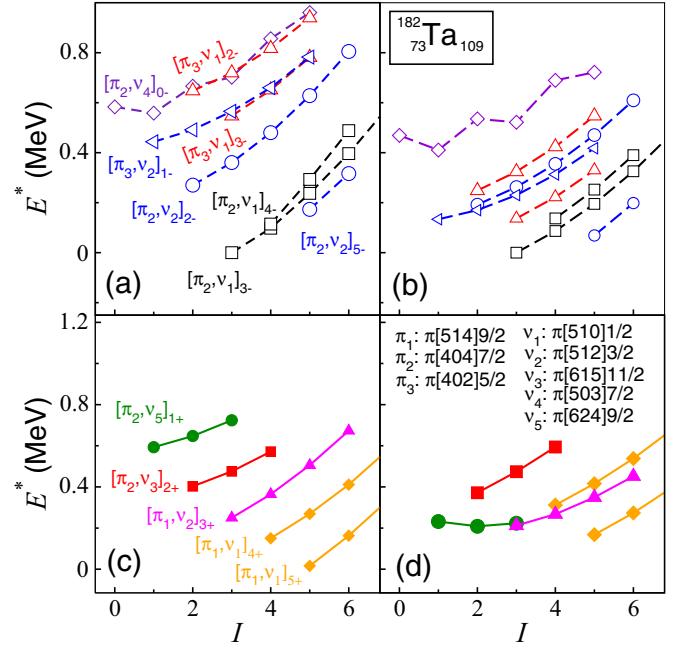


FIG. 3. Low-lying rotational bands in $^{182}\text{Ta}_{109}$. In panels (a) and (c), experimental data from [23]. In panels (b) and (d), corresponding states resulting from calculations with the Covello residual proton-neutron interaction.

experimentally observed rotational bands in ^{182}Ta . In general, the theoretical spectra for the observed bands agree quite well with experiment, although it is slightly more compressed. The calculations give the correct ground-state band based on the Nilsson states $\pi[404]7/2$ and $\nu[510]1/2$ coupled to $K^\pi = 3^-$, which is favored by the Gallagher-Moszkowski (GM) [24] rule.

The partner ($\pi[404]7/2$, $\nu[510]1/2$); $K^\pi = 4^-$ bandhead has excitation energy $E^* = 137$ keV, compared to the experimental value of 114 keV. The excitation energies of the bandheads slightly deviate compared to data with differences up to ~ 200 keV. One major source of discrepancy can be attributed to the quasiparticle energies, which are obtained from the FY mean field. This can further lead to a large Coriolis mixing if two bandhead configurations differing by $\Delta K = 1$ come close in energy. The large number of states within 1 MeV excitation energy is the main difficulty in making predictions for the low-energy structure of odd-odd nuclei. A displacement of a bandhead by ~ 100 keV can significantly change the predicted ground-state spin and parity. Another systematic discrepancy between theory and data is that the slope of calculated rotational bands is smaller than measured. This suggests that a too-large moment of inertia is used for the rotor.

Figure 4 shows low-lying $K = 0$ bands in rare-earth nuclei. The odd-even I staggering observed in $K = 0$ bands is to first order due to the Newby term in the diagonal matrix elements, that can be classified as central type for spin-singlet bandheads, or of tensor type for spin triplet bandheads [14]. The ($\pi[404]7/2$, $\nu[503]7/2$); $K^\pi = 0^-$ band in ^{182}Ta [Fig. 4(a)] and the ($\pi[404]7/2$, $\nu[633]7/2$); $K^\pi = 0^+$ band

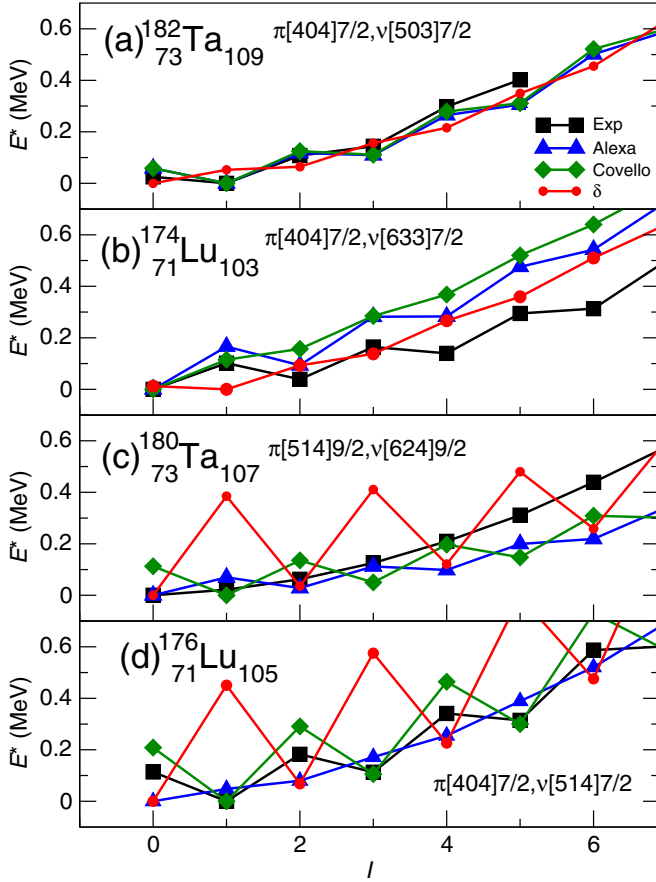


FIG. 4. Lowest-lying $K = 0$ bands in $^{174,176}\text{Lu}_{103,105}$ and $^{180,182}\text{Ta}_{107,109}$. The excitation energy E^* is here defined relative to the lowest-energy member of the band.

in ^{174}Lu [Fig. 4(b)] have bandheads dominated by spin-triplet configurations. The tensor and spin-orbit terms of the residual interaction thus contribute significantly to the diagonal matrix elements. Calculations with both the Gaussian Alexa and Covello interactions reproduce the correct phase of the staggering for these bands, although the staggering obtained with the Covello interaction for the Lu band [Fig. 4(b)] is of too-small magnitude. The δ interaction, which only has central components, on the other hand, produces staggering of opposite phase compared to experiment.

Figures 4(c) and 4(d) show the $(\pi[514]9/2, \nu[624]9/2)$ and $(\pi[404]7/2, \nu[514]7/2)$; $K^\pi = 0^-$ bands in ^{180}Ta and ^{176}Lu , respectively. The bandheads are dominated by spin-singlet configurations and are thus affected by Newby terms of central type. The experimental data for the $(\pi[514]9/2, \nu[624]9/2)$ band in Fig. 4(c) show no clear staggering, while the data for the $(\pi[404]7/2, \nu[514]7/2)$ band in Fig. 4(d) has a clear staggering with odd I lowered compared to the general trend. The δ interaction gives a large odd-even staggering inconsistent with experiment, with odd spins pushed up in energy in both cases. The Alexa interaction gives similar staggering but with smaller magnitude. The Covello interaction gives rise to a staggering with the odd spins lowered, but with a magnitude that is slightly larger than experi-

ment for the $K = 0$ band in Fig. 4(d). As expected, the results employing the Covello interaction are similar to the previous results for $K = 0$ bands in Refs. [16,25], where the same interaction is used. The quantitative agreement with experiment is not as satisfactory as in those studies, partly due to that the quasiparticle energies are not locally optimized to neighboring odd- A nuclei in the current calculations.

IV. RESULTS FOR GROUND STATES

A. Ground-state spins of odd-odd nuclei

In our comparison to data we consider only odd-odd nuclei with clear ground-state spin and parity assignments in Ref. [10]. From these cases we exclude nuclei with calculated octupole ground-state deformation $\varepsilon_3 \neq 0$ in the theoretical mass table [1]. The nuclei are classified as spherical when the ground-state ε_2 deformation in the mass table is small, $|\varepsilon_2| \leq 0.05$, and deformed if $|\varepsilon_2| > 0.05$. This selection of data gives 268 nuclei, of which 222 are considered deformed and 46 spherical. The ground-state spins for deformed nuclei are calculated using the particle-rotor model detailed in Sec. II. For the spherical nuclei, the prescription in Sec. IID is employed. The results are compared with the ground-state spins obtained using simple empirical rules as described below.

1. Empirical rules for the ground-state spin

The empirical Nordheim [26] and GM [24] rules refer to the energy order of coupled spin states in spherical and deformed odd-odd nuclei, respectively. As a simple method to determine the ground-state spin we consider the application of these rules using the lowest-energy quasiparticle states from the folded-Yukawa mean field. The parity is then determined by the parity of the proton and neutron quasiparticles.

In the spherical case, the ground state can be described as belonging to a two-quasiparticle multiplet,

$$[\beta_{j_p}^\dagger, \beta_{j_n}^\dagger]_{IM}|0\rangle, \quad (18)$$

where $\beta_{j_{p(n)}}^\dagger$ creates a proton (neutron) quasiparticle in a spherical j shell with spin $j_{p(n)}$, and the brackets denote the coupling of the spins to total angular momentum I , with projection M . The Nordheim rule states that the state where the intrinsic spins of the proton and neutron are parallel is favored (such as in the deuteron). The ground-state spin estimated with this rule is thus,

$$I = \begin{cases} j_p + j_n, & \text{if } j_p - l_p = j_n - l_n, \\ |j_p - j_n|, & \text{otherwise} \end{cases}, \quad (19)$$

where $l_{p(n)}$ is the orbital angular-momentum quantum number for the proton (neutron) quasiparticle.

For the axially deformed case, the two particles can couple as $\beta_n^\dagger \beta_p^\dagger |0\rangle$, with $K = \Omega_n + \Omega_p$, and $\beta_n^\dagger \beta_p^\dagger |0\rangle$, with $K = |\Omega_n - \Omega_p|$. Here $n(p)$ labels the neutron (proton) quasiparticle with the smallest quasiparticle energy $E_{n(p)}$. Neglecting the collective rotation and the residual proton-neutron interaction implies that these two bandheads are degenerate and the lowest in energy. This degeneracy will be broken both by the residual neutron-proton interaction and by the collective rotation. The empirical GM rule states that the bandhead with

TABLE VI. Percentage of calculated ground-state spin and parity, I^π , that agree with experimental data. The columns show agreement for different categories of nuclei: Def. (Sph.) refer to nuclei with calculated ground-state ε_2 deformations larger (smaller) than 0.05; $n \geq 3$ indicates the further restriction that three or more odd- A neighbors have correct ground states in the calculations presented in Fig. 1. The numbers in parenthesis are the total number of nuclei in each category.

Model	Def. (222)	Sph. (46)	Def. $n \geq 3$ (56)	Sph. $n \geq 3$ (28)
Empirical rules	29%	39%	54%	50%
δ	28%	37%	43%	46%
Covello	31%	41%	55%	54%
Alexa	22%	35%	45%	43%

$K = K_{\text{fav}}$, where the intrinsic spin projections of the proton and neutron are parallel is lowest in energy. This allows for a simple recipe to obtain the ground-state spin I as

$$I = K_{\text{fav}}. \quad (20)$$

The GM rule is formulated in terms of the asymptotic Nilsson quantum numbers. To avoid ambiguities when the folded-Yukawa potential mixes different Nilsson orbitals, we implement the rule using the product of the expectation values of the proton and neutron intrinsic spin projections, $f = \langle n | s_3 | n \rangle \langle p | s_3 | p \rangle$, selecting the bandhead with a positive f .

2. Agreement with ground-state spins and parities

The ground-state spins of the selected 268 odd-odd nuclei are calculated in four different ways: either using empirical rules or one of the three interactions. The results are summarized in Table VI. Applying the empirical rules, 29% of the deformed and 39% of the spherical odd-odd nuclei are predicted to have spin and parities that agree with experiment. The only nucleon-nucleon interaction that performs better than the empirical rules is the one of Covello.

In total the Covello interaction gives rise to to 33% correctly predicted ground-state spins and parities. For comparison the HFB-24 mass model [27,28] based on the Skyrme interaction gives 25% correct ground-state spins and parities for the odd-odd nuclei. However, the tabulated values from this model [28] is for a different data set of 480 odd-odd nuclei, which may affect the comparison.

The results are sensitive to the predicted quasiparticle spectrum and the agreement with data should improve if neighboring odd nuclei have correct ground-state spin assignments. To study this we consider the subset of nuclei where three or four (of the four) odd- A neighbors are predicted correctly. The agreement with data for the Covello interaction then increases from 31% to 55% for deformed, and from 41% to 54% for spherical nuclei, that is, a larger improvement for deformed nuclei. Thus, even when the neighboring nuclei are correctly assigned, implying proper quasiparticle spectra, it is still difficult to predict the level that comes lowest for the odd-odd nucleus.

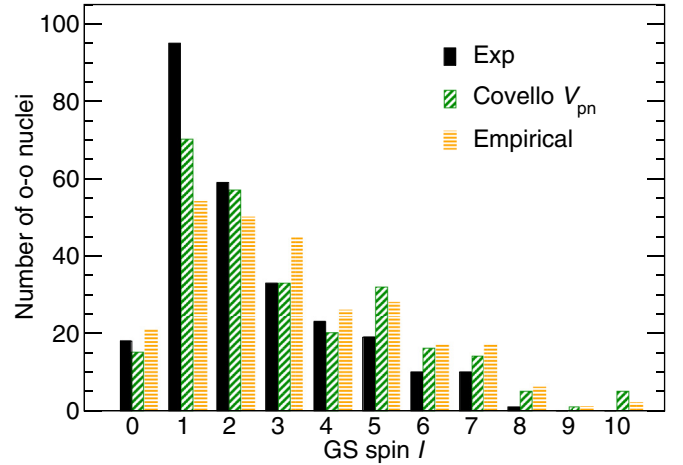


FIG. 5. Distribution of ground-state spins for the odd-odd nuclei in the data set. The data from Nubase 2016 [10] (solid bars) are compared with results from the calculations with the Covello residual interaction (striped bars) and results from using the empirical rules (horizontally striped bars).

The distribution of ground-state spins obtained with the Covello interaction is shown in Fig. 5. The distribution obtained with the microscopic treatment is substantially better than the one obtained from the empirical rules. For example, a large part of the experimental states (35%) have $I = 1$ and such ground states are predicted more often with the microscopic treatment. As seen in the figure both theoretical approaches tend to predict too many states with $I \geq 5$ and too few with $I = 1$. Presumably, a smaller moment of inertia in the rotor calculation would push up higher spins and favor lower spins and consequently increase the number of $I = 1$ ground states and decrease the number of $I = 5$ states.

The predicted ground-state spins compared to experiment are shown in Fig. 6. As seen from the figure there is a tendency for high ground-state spins to be found just above or below magic numbers that correlates with the presence of intruder shells. Interestingly, the ground-state spins for several nuclei on the $N = Z$ line tend to be $I = 0$ while in the model the interaction favors parallel coupling when the two odd particles are in the same shell.

B. Proton-neutron interaction energy for spherical nuclei

In the FRDM an additional term is added to the binding energy of odd-odd nuclei that represents the average neutron-proton interaction energy [1,29]. This average interaction energy is modeled as inversely proportional to the nuclear surface,

$$E_{pn}^{(\text{mac})} = -\frac{h}{B_s A^{2/3}}, \quad (21)$$

where B_s is ratio of the surface area of the nuclear shape to that of a sphere of the same volume. The constant h is empirically determined from mass differences to be 6.6 MeV.

The present microscopic treatment of the neutron-proton interaction energy gives fluctuations of masses of odd-odd nuclei that are not captured by traditional FRDM calculations

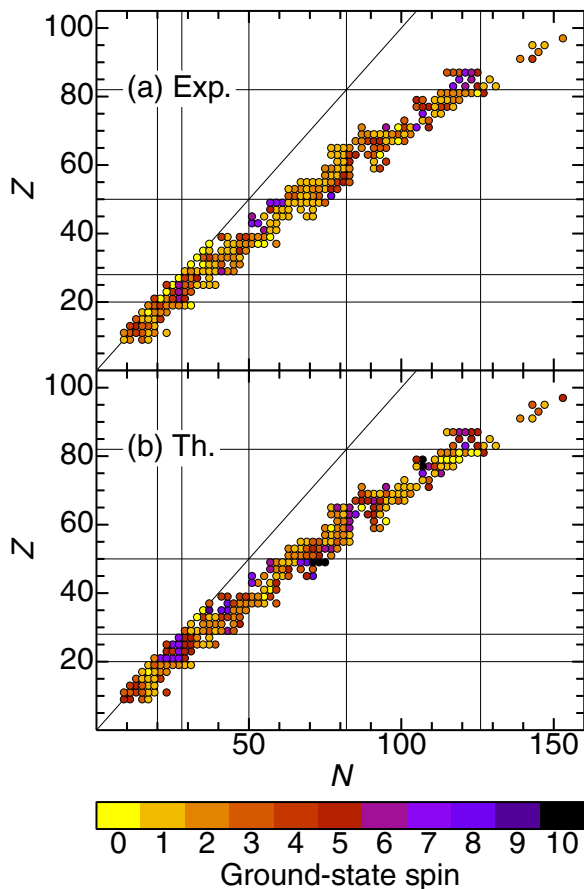


FIG. 6. Ground-state spins in odd-odd nuclei from Nubase 2016 [10] (a) compared to results with the Covello residual interaction (b).

[1]. In order to investigate if the microscopic treatment here performed leads to improvements we define a total binding energy for odd-odd nuclei as:

$$E(Z, N) = E_{\text{FRDM}} - [E_n + E_p + E_{pn}^{(\text{mac})}] + E_{\text{gs}}. \quad (22)$$

That is, we remove the contribution in the FRDM calculation [1] resulting from the quasiparticle energies $E_{n(p)}$ and their average interaction energy $E_{pn}^{(\text{mac})}$, taken from Eq. (21). Instead we add the here-calculated ground-state energy E_{gs} from the Hamiltonian (1), that includes terms for the two-quasiparticles plus rotor model with the neutron-proton interaction. For spherical nuclei E_{gs} is taken as the corrected energy E' [Eq. (17)].

In the formalism employed here the addition of an odd proton and odd neutron gives rise to both an energy contribution due to the angular-momentum coupling of the particles with the remaining core and an interaction energy between the two particles. To focus on the interaction part we consider spherical systems where our results are independent of the moment of inertia of the core.

It is interesting to investigate if the neutron-proton interactions used can give a correction to the binding energies that captures trends that the simple function, Eq. (21), does not. To enhance the contribution from the neutron-proton interaction energy we employ the nine-point mass difference formula of

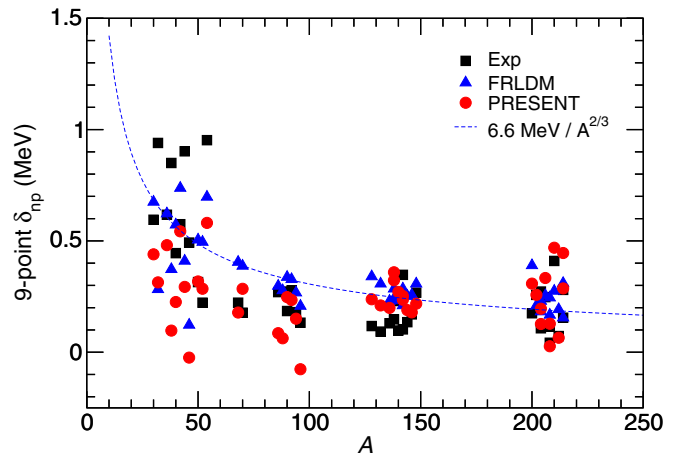


FIG. 7. Nine-point binding-energy difference δ_{np} for odd-odd spherical nuclei with known ground state I^π . The experimental data are compared with the corresponding δ_{np} obtained from the theoretical mass table and with results obtained using the microscopic model, Eq. (22).

Ref. [29] that considers all eight neighboring nuclei (four even-even and four odd-even) and the odd-odd nucleus with N, Z ,

$$\delta_{np}(Z, N) = \frac{1}{2} \sum_{N', Z' \in \text{odd-A}} E(N', Z') - \frac{1}{4} \sum_{N', Z' \in \text{even}} E(N', Z') - E(N, Z).$$

We compare the binding energy differences obtained from experiment and theory for odd-odd spherical nuclei with known ground state I^π . The theoretical masses are taken from Ref. [1] where the odd-odd mass has been adjusted according to Eq. (22) in the present microscopic calculations. The result is shown in Fig. 7. As seen in this figure the macroscopic approximation used in the FRDM captures the average trend in δ_{pn} . The microscopic results obtained with the Covello interaction gives values that are a bit too low for the lighter nuclei but otherwise describes the data with a similar accuracy.

V. Q_α VALUES OF ODD-ODD SUPERHEAVY NUCLEI

The extension of the FRDM as discussed in the previous sections gives predictions not only for ground-state spins but also for the low-energy spectra. Indeed, the low-energy spectra is important in order to determine the α -decay paths. In this section we apply the model for the prediction of how odd-odd superheavy element (SHE) may decay via α decay to ground states or to excited states.

The α decay is one of the primary decay modes of the currently known SHE. A probable scenario in experiments with odd-odd SHE nuclei is that the mother nucleus reaches its ground state before it α decays. This α decay can give a daughter nucleus in its ground state, giving the largest possible Q_α value, or leave the daughter in an excited state,

yielding a smaller Q_α . If a decay to an excited state occurs, the daughter nucleus can then γ decay. When measured in an α - γ -spectroscopy experiment, such decay events can provide valuable nuclear-structure information. In this section, we present results for Q_α values of odd-odd SHE obtained in calculations performed as in Sec. III. The Q_α values of decays connecting ground states, and the Q_α value of the favored decays connecting the mother-nucleus ground state to a structurally similar excited state in the daughter are considered. A favored Q_α smaller than the ground-state to ground-state value, but not significantly reduced, indicates a possible candidate for an α - γ event.

The branching ratio between different competing α decay paths depends on both the Q_α value and the overlap of nuclear wave functions, quantified using a hindrance factor. To fully describe the competition between different decay paths requires a microscopic calculation of the α -decay rates [30,31]. Here we consider a simple prescription to estimate the favored α -decay channel for odd-odd nuclei. The decay most favored by the nuclear structure is likely to be the case where the quasiparticle structure of the mother and daughter states are most similar. The favored decay channel is therefore selected based on the calculated mother and daughter wave

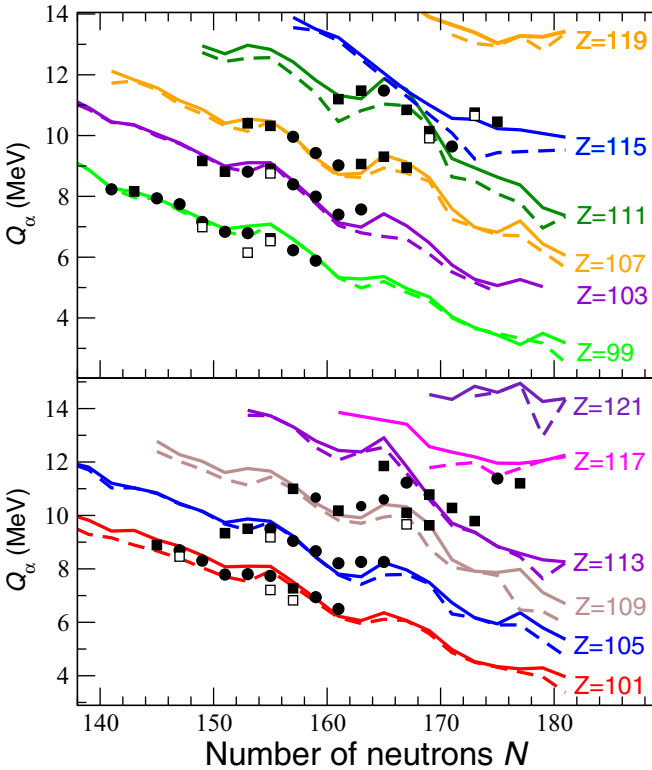


FIG. 8. Q_α values for odd-odd superheavy nuclei. The solid (dashed) lines show ground-state to ground-state (ground-state to favored) Q_α obtained in the calculations with the Covello residual interaction. The solid symbols show experimental Q_α values. Squares are used for measured values [10] and circles for values deduced from systematics [10]. In the case of several measured α -decay branches, the open symbols denote the Q_α values for the branch with smallest hindrance factor [23]. Theory shifted up 0.4 MeV.

TABLE VII. Predicted ground-state spins of superheavy nuclei compared to experiment. Experimental data from Ref. [23].

Nucleus	Covello	Experiment
${}_{99}^{248}\text{Es}_{149}$	2^-	$(2^-, 0^+)$
${}_{99}^{250}\text{Es}_{151}$	6^+	(6^+)
${}_{99}^{252}\text{Es}_{153}$	5^-	(5^-)
${}_{99}^{254}\text{Es}_{155}$	5^-	(7^+)
${}_{99}^{256}\text{Es}_{157}$	2^-	$(1^+, 0^-)$
${}_{101}^{256}\text{Md}_{155}$	1^-	(1^-)

functions. We characterize the mother nucleus gs using I^π and the dominant 2-qp configuration. The favored decay channel is approximated as the transition to the daughter state with the same I^π quantum numbers that has the same dominant 2-qp configuration.

Figure 8 shows the predicted ground-state to ground-state and ground-state to favored Q_α values for odd-odd SHE with $Z = 99$ –121 compared to available experimental data. As seen in this figure many of the trends in the experimental data are captured by the theoretical calculations. For the isotope sequences with $Z = 99, 101, 103, 105, 109, 111,$ and 115 one has observed several α -decay branches. The figure also show the branches with the smallest hindrance factors [32,33]. Branches with small hindrance factors are likely to correspond to situations where the mother and daughter are structurally similar. The calculations suggest that such decays are possible for several of the heavier nuclei.

The theoretical results in Fig. 8 have been shifted up in energy by 0.4 MeV in order to better illustrate the agreement for the kinks in the Q_α values. The agreement for the kinks indicate that the shellstructure is predicted correctly while the improved agreement obtained when the values are slightly shifted could be an indication of a missing trend in the macroscopic part of the FRDM. In particular one should note that the Coulomb redistribution energy is treated only to first order in the FRDM. Since this contribution is particularly large for the nuclei considered here, which have the highest $Z^2/A^{1/3}$ of all known nuclei, higher-order or exact treatments may be required. The favorable effect on nuclear masses of already including the first-order treatment is discussed in Ref. [34].

The predicted kinks in Q_α values occurs for all chains around neutron numbers 152 and 162 and are in agreement with experiments. For the $Z = 103$ –109 chains there is a predicted kink also around neutron number 174. The kinks are indicative of shell gaps and a more detailed comparison between different models can be found in Ref. [35].

Table VII shows a comparison between the predicted I^π values for some of the nuclei in the superheavy region that have tentative I^π assignments [23]. Of the six values for the $Z = 99$ and $Z = 101$ chains, theory and experiment agree in four cases.

VI. CONCLUSIONS

We investigated how well global low-energy properties of odd-odd nuclei can be described in the FRDM combined

with the particles-plus-rotor-model. The rotor model accounts for the spin coupling and the neutron-proton interaction between the two odd particles. Different forms and parametrizations of the neutron-proton interaction were investigated, where the Gaussian interaction with central and noncentral tensor parts was found superior in the parametrization given by Covello *et al.* [16].

Bandhead energy splitting was studied in deformed nuclei between the two bandheads that emerge as the angular momentum of the odd neutron and odd proton couple to $K_> = K_n + K_p$ and $K_< = |K_n - K_p|$. Best rms deviation between data and calculation for all 54 measured cases was found to be 66 keV for the Covello interaction.

The structure of neutron-proton $j_n j_p$ multiplets in spherical nuclei could be fairly well described by the model. The noncentral tensor component of the interaction result in more correct multiplet splittings by pushing the $K = 0$ states higher in energy.

We also studied how well the model performs in the calculations of rotational bands in deformed nuclei, formed by one proton and one neutron in specified Nilsson configurations. Several low-energy bands appear, and errors up to 200 keV in the predictions (in the example of ^{182}Ta) may imply difficulties in the prediction of correct ground-state configuration.

A global study was performed of observed ground-state spins in odd-odd nuclei, where 268 observed nuclei with experimentally reliable spin and parity assignments were

compared to calculations. The conclusion is that empirical rules result in 29% correct ground-state parities and spins for spherical nuclei and 38% for deformed nuclei, while the corresponding numbers for the interaction from Covello are 31% and 41%, respectively. The microscopic calculations only implies a quite modest improvement in the prediction of ground-state spin and parity of odd-odd nuclei. However, the treatment with a residual interaction also gives bandhead splittings and more detailed spectroscopic predictions.

We finally applied the model for the description of low-energy spectra for odd-odd superheavy nuclei. From the calculated structure of the states in the mother nucleus and the daughter nucleus we could provide predictions of Q_α values for decay to both favored states and to ground states. We believe these results can be used as a reference in future experiments on superheavy nuclei.

ACKNOWLEDGMENTS

B.G.C. and S.Å. thank the Knut and Alice Wallenberg Foundation (Grant No. KAW 2015.0021) for financial support. D.W. acknowledges visits to the theory division in Los Alamos and P.M. visits to mathematical physics division in Lund. We are grateful to I. Ragnarsson for important comments on the manuscript.

-
- [1] P. Möller, A. J. Sierk, T. Ichikawa, and H. Sagawa, *At. Data Nucl. Data Tables* **109**, 1 (2016).
- [2] L. Bonneau, P. Quentin, and P. Möller, *Phys. Rev. C* **76**, 024320 (2007).
- [3] P. Möller, J. R. Nix, and K.-L. Kratz, *At. Data Nucl. Data Tables* **66**, 131 (1997).
- [4] M. T. Mustonen, T. Shafer, Z. Zenginerler, and J. Engel, *Phys. Rev. C* **90**, 024308 (2014).
- [5] W. Almosly, B. G. Carlsson, J. Suhonen, J. Toivanen, and E. Ydrefors, *Phys. Rev. C* **94**, 044614 (2016).
- [6] P. Möller and J. R. Nix, *Nucl. Phys. A* **520**, c369 (1990).
- [7] A. Bohr and B. R. Mottelson, *Nuclear Structure Vol. II* (W. A. Benjamin, New York, 1975).
- [8] B. G. Carlsson and I. Ragnarsson, *Phys. Rev. C* **74**, 044310 (2006).
- [9] I. Ragnarsson and P. B. Semmes, *Hyp. Int.* **43**, 423 (1988).
- [10] G. Audi, F. G. Kondev, M. Wang, W. J. Huang, and S. Naimi, *Chin. Phys. C* **41**, 030001 (2017).
- [11] P. Möller, R. Bengtsson, B. G. Carlsson, P. Olivius, and T. Ichikawa, *Phys. Rev. Lett.* **97**, 162502 (2006).
- [12] P. Ring and P. Schuck, *The Nuclear Many-Body Problem*, 1st ed. (Springer-Verlag, New York, 1980).
- [13] R. Bengtsson and S. Åberg, *Phys. Lett. B* **172**, 277 (1986).
- [14] J. P. Boisson, R. Piepenbring, and W. Ogle, *Phys. Rep. C* **26**, 99 (1976).
- [15] P. Alexa, J. Kvasil, N. V. Minh, and R. K. Sheline, *Phys. Rev. C* **55**, 179 (1997).
- [16] A. Covello, A. Gargano, and N. Itaco, *Phys. Rev. C* **56**, 3092 (1997).
- [17] G. Ehrling and S. Wahlborn, *Phys. Scr.* **6**, 94 (1972).
- [18] P. C. Sood, D. M. Headly, R. K. Sheline, and R. W. Hoff, *At. Nucl. Dat. Table* **58**, 167 (1994).
- [19] N. D. Newby, Jr., *Phys. Rev.* **125**, 2063 (1962).
- [20] B. G. Carlsson and J. Toivanen, *Phys. Rev. C* **89**, 054324 (2014).
- [21] A. V. Afanasjev and E. Litvinova, *Phys. Rev. C* **92**, 044317 (2015).
- [22] D. Tarpanov, J. Dobaczewski, J. Toivanen, and B. G. Carlsson, *Phys. Rev. Lett.* **113**, 252501 (2014).
- [23] NNDC database, <https://www.nndc.bnl.gov>.
- [24] C. I. Gallagher and S. A. Moszkowski, *Phys. Rev.* **111**, 1282 (1958).
- [25] A. Covello, A. Gargano, and N. Itaco, *Phys. Rev. C* **65**, 044320 (2002).
- [26] L. W. Nordheim, *Phys. Rev.* **78**, 294 (1950).
- [27] Goriely *et al.*, *Phys. Rev. C* **88**, 024308 (2013).
- [28] HFB-24 mass formula, <http://www.astro.ulb.ac.be/pmwiki/Brusslib/Hfb17>.
- [29] D. G. Madland and J. R. Nix, *Nucl. Phys. A* **476**, 1 (1988).
- [30] D. E. Ward, B. G. Carlsson and S. Åberg, *Phys. Rev. C* **88**, 064316 (2013).
- [31] D. E. Ward, B. G. Carlsson, and S. Åberg, *Phys. Rev. C* **92**, 014314 (2015).
- [32] D. Rudolph *et al.*, *Phys. Rev. Lett.* **111**, 112502 (2013)
- [33] D. Rudolph, L. G. Sarmiento, and U. Forsberg, *AIP Conf. Proc.* **1681**, 030015 (2015).
- [34] P. Möller, J. R. Nix, W. D. Myers, and W. J. Swiatecki, *Nucl. Phys. A* **536**, 61 (1992).
- [35] P. Jachimowicz, M. Kowal, and J. Skalski, *Phys. Rev. C* **89**, 024304 (2014).